Noncolocated Structural Vibration Suppression Using Zero Annihilation Periodic Control

David S. Bayard
Jet Propulsion laboratory, MS T-1711
California Institute of Technology
4800 Oak Grove Drive
Pasadena, CA 91109

Tel: (818) 354-8208
e-mail: bayard@bert2.jpl.nasa.gov

and

Dhemetrios Boussalis
Jet Propulsion Laboratory, MS T-1711
California Institute of Technology
4800 Oak Grove Drive
Pasadena, CA 91109

Tel: (818) 354-3977
e-mail: boussali@taurus.jpl.nasa.gov

Keywords: Periodic control, noncolocated systems, non-minimum phase, zero annihilation, flexible structures, vibration suppression.

NO NCOLOCATED STRUCTU RAL VIBRATION SUPPRESSION USING ZE RO ANNIHILATION PERIODIC CO NTROL

David S. Bayard and Dhemetrios Boussalis
Jet Propulsion Laboratory
California Institute of Technology
4S00 Oak Grove Drive
Pasadena, CA 91109

ABSTRACT

The Zero Annihilation Periodic (ZAP) controller is applied to the problem of vibration control of a noncolocated flexible structure. 1 t is shown that even though the transfer function is nonminimum-phase, a plant inverse controller can be designed which elicits a deadbeat closed-loop response. The transfer function under investigation arises from a noncolocated actuator/sensor configuration used on the ASTREX flexible structure at USAF/Phillips Laboratory. Several simulation examples are given to demonstrate the ZAP control method. As expected from the theory, the closed-loop response is deadbeat, and the vibrations are damped instantaneously.

1. 1NTROIIUC'I'1ON

The Zero Annihilation Periodic (ZAP) control law was introduced in Bayard [3] [4] [5] for controlling nonminimum phase systems using stable plant inversion. The general approach is based On the notion of a mathematical '(lifting" in which a serial-to-parallel conversion is performed on the plant input and output signals, and mappings arc considered bet ween the vectorized quantities. Bayard's lifting [5] is a generalization of Lozano's lifting [10] to the extended horizon case. The generalization to the extended horizon case is crucial for control gain reduction in order to allow practical implementations of the approach.

A key property of the above liftings which makes thcm so useful is that the transmission zeros of the lifted plant arc annihilated (i.e., placed to the origin). This zero- annihilation (2A) property allows the lifted plant to be stably inverted using standard control methods. This result is important to many areas of control, communications, and signal processing where a stable plant inverse is often desired but not possible due to nonminimum- phase restrictions.

In the present paper, the extended horizon ZAP controller is applied to the problem of vibration control of a nonminimum-phase transfer function. The transfer function arises from a noncolocated actuator/sensor configuration used on the ASTREX facility at the USAF/Phillips Laboratory, Edwards Air Force Base [1 1]. Several simulation examples arc given to demonstrate the ZAP control method. As expected from the theory, the closed-loop response is deadbeat, and the vibrations arc damped instantaneously.

'2. BACKGROUND ANI) NOTATION

Consider the input/output model,

$$\mathcal{A}(z^{-1})y_\ell = \mathcal{B}(z^{-1})u_\ell \tag{2.1a}$$

$$\mathcal{A}(z^{-1}) = 1 + \sum_{i=1}^{n} a_i z^{-i}; \qquad \mathcal{B}(z^{-1}) = \sum_{i=1}^{n} b_i z^{-i} \tag{2.1b}$$

where polynomials $\mathcal{A}$ and $\mathcal{B}$ are assumed to be relatively prime. It is assumed that $b_1 \neq 0$, so that the polynomial $\mathcal{B}$ can be factored uniquely into the form $\mathcal{B}(z^{-1}) = z^{-d} b_1 \bar{\mathcal{B}}(z^{-1})$ where $\bar{\mathcal{B}}(z^{-1})$ is monic and $d = 1$ is the plant delay. It is desired to transform (2.1) into the Block Multirate Input/Output form of Albertos [I], for which it will be necessary to make the following assumptions,

A.1 The plant delay is known (and given by $d = 1$)

A.2 An upper bound $\bar{n} \geq n$ is known on the plant order n

The choice $d = 1$ *in* assumption A.1 is for convenience only and is not a fundamental restriction. In the case that $d \neq 1$, knowledge of d ensures that all subsequent expressions can be appropriately modified without loss of generality.

Choose some horizon time N > $\bar{n}$. The system (2.1) is iterated to give the following system of linear equations,

$$\text{Y(k)} = A_1 Y(k) + A_2 Y(k-1) + \text{Ill U(k)} + B_2 U(k-1) \tag{2.2}$$

where,

$$\text{Y(k)} = \begin{bmatrix} y_{kN+1} \\ y_{kN+2} \\ \vdots \\ y_{kN+N} \end{bmatrix}; \qquad U(k) = \begin{bmatrix} u_{kN} \\ u_{kN+1} \\ \vdots \\ u_{kN+N-1} \end{bmatrix} \tag{2.3}$$

A_1 = lower triangular Toeplitz, with first column $[0, -a_1, \ldots, -a_n, 0, \ldots 0]^T$

A_2 = upper triangular Toeplitz, with first row $[0, \ldots 0, -a_n, \ldots -a_1]$

B_1 = *lower* triangular- Toeplitz, with first column $[b_1, b_2, \ldots b_n, 0, \ldots 0]^T$

B_2 = upper triangular Toeplitz, with first row $[0, \ldots 0, b_n, \ldots b_2]$

It is convenient to combine terms involving Y(k) in (2.2) and rearrange to give the following input/output characterization,

Block Multirate Input/Output (BMIO) Representation

$$Y(k) = AY(k-1) + HU(k) + BU(k-1) \tag{2.4}$$

where,

$$A = (I - A_1)^{-1} A_2 \tag{2.5a}$$

$$H = (I - A_1)^{-1} B_1 \tag{2.5b}$$

$$B = (I - A_1)^{-1} B_2 \tag{2.5c}$$

Several advantages anti properties of the BMIO representation are discussed in Albertos [1]. It is noted that since A_1 is lower triangular with zeros on the diagonal, the quantity $(I - A_1)$ is always invertible. Hence the quantities in (2.5) always exist, and the BMIO model (2.4) is a first order vector ARX process which is equivalent to the original system (2.1). It is emphasized that only assumptions A. 1 and A.2 were required to put the plant into the desired BMIO form.

Polynomial $\mathcal{A}$ is divided into $\mathcal{B}$ to give impulse response sequence $\{h_i\}$,

$$\frac{\mathcal{B}(z^{-1})}{\mathcal{A}(z^{-1})} = \sum_{i=1}^{\infty} h_i z^{-i} \tag{2.6}$$

The quantities *hi* are referred to as Markov parameters. The impulse response sequence $\{h_i\}$ is not assumed to be convergent (i.e., the system may be unstable). Using the Toeplitz structure of A_1 and B_1 and relation (2.6), it can be shown [1] *[3]* that the matrix H in (2.4) (2.5b) can be written in terms of the Markov parameters as,

$$H = \begin{bmatrix} h_1 & 0 & \cdots & 0 \\ h_2 & h_1 & \ddots & \vdots \\ \vdots & \ddots & \ddots & 0 \\ h_N & \cdots & h_2 & h_1 \end{bmatrix} \tag{2.7}$$

This is the desired expression for H, i.e.,

H = lower triangular Toeplitz, with first column $[h_1, h_2, \ldots, h_N]^T$

Since the delay is unity by assumption (i.e., $d = 1$), the matrix H has a nonzero diagonal *(i.e.,* $h_1 \neq 0$), and is always invertible.

3. GENERALIZED LIFTINGS

In this section, a class of generalized liftings wil' be defined from the BM1O plant representation (2.4).

Some new notation is required at this point. In general, consider some vector $V \in R^N$. Then a *partial horizon* vector $V_s = SV$ is defined where $S \in R^{\sigma \times N}$ is a *selection matrix* which selects $\sigma \leq N$ components of V for inclusion in $V_s \in R^{\sigma}$. For this purpose, S will be a matrix of O's and 1's with a a single "l" in every row, and a single "l" in only σ of its N columns.

As indicated by the expression $V_s = SV$, the subscript '(s" will be used throughout to denote quantities which are constructed from "selected" elements of their unsubscripted counterparts.

The selection matrix S defined above can also be thought of as being specified uniquely by a (), 1 *window vector* $\rho = [\rho_1, \ldots, \rho_N]$ whose entries are,

$$\rho_i = \begin{cases} 1 & \text{if } i\text{th entry of } V \text{ is included in } V_s \\ 0 & \text{otherwise} \end{cases}$$

The number of "1 'S" in ρ is defined as σ. Note that if the elements of ρ were to be plotted versus their index, a O, 1 "window" is formed over the N-step horizon, depicting which σ components of V are to be included in V_s. The construction of S from ρ in this manner defines a one-to-one mapping $S = W(p)$ which will be convenient notation in the paper.

As an example, consider the plot shown in Fig. 1 for an input window ρ_u and an output window ρ_y. The construction of selection matrices S_u and S_y corresponding to the windows ρ_u and ρ_y in Fig. 1, is shown in the example below.

Example 1 Consider the case in Fig. 1 where N = 6, and $\rho_y = [0,0,1,1,1,0]$, $\rho_u = [0,1,1, 1,0,0]$. Then, $\sigma_y = \sigma_u = 3$, $\rho_y^c = [1,1, 0,0,0, 1]$ (the *complementary* window to ρ_y) and,

$$S_u = \mathcal{W}(\rho_u) = \begin{bmatrix} 0 & 1 & 0 & 0 & 0 & 0 & 0 \\ 0 & 0 & 1 & 0 & 0 & 0 & 0 \\ 0 & 0 & 0 & 1 & 0 & 0 & 0 \end{bmatrix}$$

$$S_y = \mathcal{W}(\rho_y) = \begin{bmatrix} 0 & 0 & 1 & 0 & 0 & 0 & 0 \\ 0 & 0 & 0 & 1 & 0 & 0 & 0 \\ 0 & 0 & 0 & 0 & 1 & 0 & 0 \end{bmatrix}$$

$$S_y^c = \mathcal{W}(\rho_y^c) = \begin{bmatrix} 1 & 0 & 0 & 0 & 0 & 0 & 0 \\ 0 & 1 & 0 & 0 & 0 & 0 & 0 \\ 0 & 0 & 0 & 0 & 0 & 0 & 1 \end{bmatrix}$$

Note that in the example, we have included the selection matrix S_y^c associated with the window ρ_y^c which is defined as the O-1 complement of window ρ_y. This complementary window will play an important role in the following discussion.

Using the above notation, the following partial horizon vectors will be used in the paper,

$$Y_s(k) \triangleq S_y Y(k); \quad S_y \triangleq \mathcal{W}(\rho_y) \in R^{\sigma_y \times N}$$

$$U_s(k) \triangleq S_u U(k); \; S_u \triangleq \mathcal{W}(\rho_u) \in R^{\sigma_u \times N}$$

$$Y_s^c(k) \triangleq S_y^c Y(k); \; S_y^c \triangleq \mathcal{W}(\rho_y^c) \in R^{(N-\sigma_y)\times N}$$

where ρ_y and ρ_u are specified O, 1 window vectors, and ρ_y^c is defined as the O, 1 complement of ρ_y. Intuitively, Y_s^c is a vector comprised of all elements of the vector Y which are not included in Y_s.

A general class liftings is now defined from the BMIO plant representation (2.4) by making the input nonzero only over a restricted portion of each horizon, and by measuring the output only over a restricted portion of each horizon. Specifically, the partial horizon input and outputs defined above are used in the BMIO model (2.4) to give,

$$\begin{bmatrix} Y(k) \\ U_s(k) \end{bmatrix} = \begin{bmatrix} A & BS_u^T \\ 0 & 0 \end{bmatrix} \begin{bmatrix} Y(k-1) \\ U_s(k-1) \end{bmatrix} + \begin{bmatrix} HS_u^T \\ I \end{bmatrix} U_s(k) \tag{31}$$

$$Y_s(k) = [S_y \quad 0] \begin{bmatrix} Y(k) \\ U_s(k) \end{bmatrix} \tag{3.2}$$

It, is shown in [5] that the lifted plant (3.1)(3.2) can be transformed by similarity to the following more useful form,

Generalized Lifting System Model

$$\begin{bmatrix} Y_s(k) \\ Y_s^c(k) \\ U_s(k) \end{bmatrix} = \begin{bmatrix} S_y A S_y^T & S_y A (S_y^c)^T & S_y B S_u^T & Y_s(k \\ S_y^c A S_y^T & S_y^c A (S_y^c)^T & S_y^c B S_u^T & Y_s^c(k-1) \\ o & 0 & 0 & U_s(k-1) \end{bmatrix} \quad 1)$$

$$+ \begin{bmatrix} S_y H S_u^T \\ S_y^c H S_u^T \\ 1 \end{bmatrix} U_s(k) \tag{3.3}$$

The lifted system model (3.3) is depicted in the block diagram of Fig. 2. It is seen that Y_s and Y_s^c form two coupled subsystems which arc driven by a common input U_s. It is also noted that the transmission zeros of the transfer function from $U_s(k)$ to $Y_s(k)$ arc affected by the choice of windows $p.$ and ρ_y. This is a kcy feature of the lifted systcm model which will be used to advantage in later developments.

It is noted that the liftings are defined uniquely by the choice of selection windows ρ_u and ρ_y. An important class of liftings will be defined in the next section.

4. EXTENDED HORIZON LIFTINGS

Consider the class of liftings defined by Bayard in [5],

Extended Horizon Liftings

$$\rho_u = [\overbrace{0,\ldots,0}^{m}\overbrace{1,\ldots,1}^{\ell},\overbrace{1,\ldots,1}^{n},\overbrace{0,\ldots,0}^{n}] \tag{4.1a}$$

$$\rho_y = 0[\overbrace{0,\ldots,0}^{m}\overbrace{0\ldots0}^{\ell}\overbrace{\ldots\ldots}^{n}\overbrace{0,1,\ldots,1}^{n}] \tag{4.1b}$$

where $\ell \geq$ O, $m \geq o$, and $n > 0$ is the order of the irreducible plant (2.1). Note that the total horizon length is given by N $= m + \ell +$ 2n. This is denoted as an extended horizon lifting because N is greater than $2n$ where n is the order of the plant.

Remark 1 The Lozano lifting [10] corresponds to a lifting where the horizon length N is exactly $2n$, and the lifted plant is square (i. e., $\sigma_u = \mathrm{cr}_y$). In comparison, the Extended Horizon liftings allow N >271 where the extra degrees of freedom will be used to advantage.

Remark 2 It is noted that if one chooses $m > 0$ in (4.1), the first control action is not applied until m + 1 sample times into the window. Hence, the extra 7n $* T$ seconds of free time can be used to perform computations (where T is the sampling interval). Since m can be chosen arbitrarily in this lifting, the dead time can be matched to the real-time computer requirements.

Remark 3 If one chooses $\ell > 0$ in (4.1), there are more control inputs than outputs in the lifted system (i. e., $\sigma_u > \sigma_y$). It will be seen that these extra degrees of freedom in the input can be used to advantage to minimize a quadratic control cost and hence reduce control gains significantly compared with the case $\ell = 0$.

It has been shown in Bayard[5] that the following conditions are satisfied by the extended horizon lifting (4.1),

Output Tracking (O T) Condition

$$H_s H_s^{\dagger} = I \tag{4.2}$$

Zero Annihilation (2A) Conditions

$$BS_u^T = 0 \tag{4.3a}$$

$$A(S_y^c)^T = 0 \tag{4.3b}$$

Substituting the ZA conditions *(4.3)* into *(3.3) gives* the simplified system model,

Extended Horizon Lifting System Model

$$Y_s(k) = S_y A S_y^T Y_s(k-1) + H_s U_s(k) \tag{4.4a}$$

$$Y_s^c(k) = S_y^c A S_y^T Y_s(k-1) + S_y^c H S_u^T U_s(k) \tag{4.4b}$$

where "selected" matrix H_s is defined as,

$$H_s = S_y H S_u^T \tag{4.5}$$

Equivalently, under the ZA conditions the system shown in Fig. 2 simplifies to the system shown in Fig. 3. All of the key properties of the extended horizon lifting (4.1) can be understood by comparing Fig. 2 and Fig,. 3, It is noted that Y_s^c no longer couples into the Y_s subsystem. Furthermore, the Y_s^c subsystem has become deadbeat i.e., all of the poles of the Y_s^c subsystem are at the origin. Most importantly, (assuming H_s is square), *the transmission zeros of the transfer function from $U_s(k)$ to Y.(k) have been annihilated (i. e.,* placed at the origin). If H_s is not square, the transmission zeros of the "squared down" transfer function from V (where $U_s = H_s^{\dagger} V$) to Y_s are annihilated.

5. ZERO ANNIHILATION PERIODIC (ZAP) CONTROL

The placement of the transmission zeros to the origin by the extended horizon lifting (4 .1) allows stable invertibility of the transfer function from $U_s(k)$ to $Y_s(k)$. The *ZAP* control law which will be discussed next deadbeats the response $Y_s(k)$ to follow the desired $Y_d(k)$, subject to the minimization of a quadratic control cost.

To derive the ZAP controller, define the output error as,

$$E(k) = Y_d(k) - S_y Y(k) \tag{1.1}$$

Substituting (2.4) into (4.1), and using (3.2) and (3.12) gives,

$$E(k) = -S_y A Y(k-1) - H_s U_s(k) + Y_d(k) \tag{5.2}$$

$$= -S_y A S_y^T Y_s(k-1) - H_s U_s(k) + Y_d(k) \tag{5.3}$$

Consider the problem of forcing the error in (5.3) to zero in a single step, while minimizing a quadratic control cost penalty, i.e. ,

$$\min_{U_s(k)} \; U_s^T(k) U_s(k) \tag{5.4a}$$

subject to

$$E(k) = 0 \tag{5.4b}$$

in light of the OT condition (4.2), this minimization problem can be solved uniquely to give the ZAP control,

Zero Annihilation Periodic (ZAP) Control Law

$$U_s^\circ(k) = H_s^\dagger \left(-S_y A S_y^T Y_s(k-1) + Y_d(k) \right) \tag{5.5}$$

$$= K^\circ Y_s(k-1) + L^\circ Y_d(k) \tag{5.6}$$

where the corresponding feedback gains are defined as,

$$K^\circ = -H_s^\dagger S_y A S_y^T \tag{5.7a}$$

$$L^\circ = H_s^\dagger \tag{5.7b}$$

Here the superscript "o" is chosen to emphasize the fact that the control nulls (i. e., deadbeats) the output, and superscript "†" denotes the Moore- Penrose pseudo-inverse (cf., Barnett [2]). ∎

For convenience the ZAP control law is summarized in the block diagram of Fig. 4. It is shown in Bayard [5] that the ZAP controller enjoys the following properties,

1. The quadratic control cost (5.4a) is minimized at each stage, subject to the deadbeat tracking constraint (5.4 b),

2. All closed-loop poles are at the origin (i.e., the closed-loop response is deadbeat), and hence $Y_s(k)$ converges to $Y_d(k)$ in a single step,

3. The closed-loop system is internally stable (e.g., $Y_s^c(k)$ remains bounded),

Remark 4 As mentioned earlier, the Lozano lifting corresponds to a case where N = 2n, σ_u = n, $sigma_y$ = n. However, in this case the lifted plant is square, and there are no surplus inputs to minimize the quadratic cost (5.4a) while satisfying the deadbeat condition (5.4 b). Hence, the control gains and input control torques associated with Lozano's approach tend to be significantly larger compared to the extended horizon case. For example, in the simulation study to follow, it will be seen that a square lifting leads to peak torques 4 *orders of magnitude larger* than the corresponding extended horizon lifting.

6. ASTREX l"AC11,I'1'%

The algorithm is now evaluated by simulation using the dynamic 1110(1 ('1 of the testbed at the U. S. A.I ('. /Phillips Laboratory's Advanced Space structures Technology Research EXperiments (ASTREX) facility. The performance assessment scenario concentrates on vibration suppression of the secondary mirror using the piezoelectric sensing/actuation embedded in the "smart strut" tripod, where it has been found that all transfer functions exhibit nonminimum phase characteristics. A brief description of the structure is given in the following.

The ASTREX facility is located at the U.S. Air Force Phillips laboratory, Edwards AFB, California, and is a testbed intended for experiments to validate methodologies and algorithms large angle slewing and vibration control of flexible space platforms [1 I]. It is an antenna-like structure (Figure 5) and consists of a pivoting test article that is mounted on an air-bearing vertical pedestal. The test article is divided into three main sections. The largest Section is the primary. Six triangular plates are mounted on the primary truss to generate moment of inertia equivalent to that of a 5-meter reflector. In addition, two cylindrical masses have been attached to opposite ends of the primary to represent the inertia of two tracking telescopes. The rear section, the tertiary, is used to house the system electronics as well as to balance the structure. Finally, the front section, the secondary, is connected to the primary through a tripod support structure. The secondary consists of three small plates that are fitted in a triangular shape. A reaction wheel is located within the triangular plate structure, while, many types of sensors can be mounted externally.

A high fidelity finite element model ha.. been generated by the Phillips Laboratory that consists of nearly 550 nodes and 1000 elements. Based on this model, a state space representations of the system can be derived for usc in design and simulation work.

Of interest in the present paper is the active strut tripod supporting the secondary. The piezoelectric actuators and sensors in the tripod are to be used with the control algorithm to effect vibration suppression. A six mode two-input two-output continuous-time state space representation {A, B, C, D} has been generated from the original finite element model that results in the frequency domain input-ouput relation

$$y(s) = [C(sI - A)^{-1}B + D]\, u(s) \qquad (6.1)$$

where $y, u \in \mathcal{R}^2$ and the matrices A, B, C and D arc of appropriate dimensions. All four transfer functions in (6.1) arc nonminimum phase as is evident from the pole-zero locations in Figures 6-9.

Since the controller is in discrete-time, the plant is digitized with a sampling interval of $T = 25\,msec$. The resulting discrete state space representation $\{\Phi, G, C, D\}$ leading to the transfer matrix relation

$$y(z) = [C(zI - \Phi)^{-1} G + D]\, u(z) \qquad (6.2)$$

with dimensions corresponding to those in (6.1). Furthermore, G, C and D are partitioned as

$$g = [g_1 g_2] \quad C = \begin{bmatrix} c_1^T \\ c_2^T \end{bmatrix} \quad D = \begin{bmatrix} d_{11} & d_{12} \\ d_{21} & d_{22} \end{bmatrix}$$

For the SISO simulations of the following section, the (1-1) channel is chosen, represented by the transfer function

$$\frac{y_1(z)}{u_1(z)} = c_1^T(zI - \Phi)^{-1}g_1 + d_{11} \tag{6.3}$$

which also possesses nonminimum phase characteristics, since tiler'c are open loop zeros outside the unit circle (Figure 1 O). For the purposes of this paper, a further simplification of the model is made by setting $d = O$. This *is* done because our existing software was developed for systems with unit delay. The algorithm, however, is valid for any delay, and the software will be upgraded in the near future. As seen from the pole-zero locations in Figure 11, this represents no serious loss of generality since the system with $d = 0$ retains the nonminimum phase characteristics.

The input and ouput of the plant arc measured in terms of the voltage in the PZT strut, and must remain within the range of $\pm 10 Volts$.

'7. SIMULATION RESUTLS

The objective of this evaluation is to demonstrate the capability of the ZAP control algorithm to effect stable plant inversion on an existing physical system (the ASTREX testbed) and, perhaps the most important contribution of this algoritm, the extended horizon lifting, that allows for adjustment of the required control effort levels by varying the partial horizon length ℓ.

The open-loop output time response of the system to a nonzero initial condition is shown in Figure 12. The closed loop simulations are run for three different partial horizon lengths $\ell =$ O, 16,40. The special case of the ZAP control law for $\ell =$ O (i.e., a square lifting) results in the closed loop ouput time response of Figure 13. This case corresponds to N $= 2n, \sigma_u =$ n, σ_y which is a square lifting analogous to that of Lozano [1 O]. Although the system exhibits deadbeat response, the applied control force induces an extremely large (order 10^4) transient amplitude. Figure 14 shows the corresponding control input plot. In this case, both input ancl output exceed the PZT strut tolerance of $\pm 10 Volts$.

When the horizon length is increased to 16 samples, the required control force is drastically reduced (Figure 15). The ouput, however, still reaches relatively high amplitude during the $1.6\,sec$ that the input is applied (Figure 16). Further increase in the horizon length $\ell =$ 40, results in the time response shown in Figures 17-18. The 12 system states (Figures 19-21) exhibit similar deadbeat behavior implying that internal stability is also maintained.

8. CONCLUSIONS

The Zero Annihilation Periodic (ZAP) controller has been applied to the problem of vibration control on the ASTREX structure model. The ZAP controller is a plant inverse control law which elicits a deadbeat closed-loop response, even though the selected transfer function was xiollnlil~ixzlur[]-phase (i.e., had zeros outside the unit circle). Several simulation runs were performed, and as expected from the theory, the closed-loop response was deadbeat, and the vibrations were damped instantaneously.

From the results of this is study, it, appears that the periodic control approach can be made feasible for vibration damping problems. Accordingly, it, is expected that the ZAP controller will be applicable to many other problem s ill acou stics, noi se reduction, flexible structures control, vi bration suppression, vibration isolation, fast, slewing, etc., where it is useful to dampen vibrations instantaneously in a d eadbeat ma n n er. The ZAP controller can also be applied to tracki ng problems which will be reported elsewhere. Future research is aimed at multivariable and adaptive formulations of periodic control approaches.

ACKNOWLEDGEMENTS

The research described in this paper has been performed at the Jet Propulsion Laboratory, California Institute of Technology, under contract with the National Aeronau tics and Space Administration.

REFERENCES

[1] P. Albertos, "Block multirate input-output model for sampled-data control systems," IEEE Trans. Automatic Control, vol. 35, no. 9, pp. 1085-1088, September 1990.

[2] S. Barnett, *Matrices: Methods and Applications.* Clarendon Press, oxford England, 1990.

[3] D.S. Bayard, "Globally stable adaptive periodic. control," Jet l'repulsion Laboratory, Internal Document JPL D-9448, February 3, 1992.

[4] D.S. Bayard, "Zero annihilation methods for direct adaptive control of nomninimurn-phase systems," in *Proc. Seventh Yale Workshop on Adaptive and Learning Systems,* Yale University, May 1992.

[5] D.S. Bayard, "Extended horizon liftings for stable inversion of nonminimum-phase systems," Jet l'repulsion Laboratory, Internal Document, in preparation.

[6] E.J. Davison and S.H. Wang, "Properties and calculation of transmission zeros of linear multivariable systems," Automatic, Vol. 10, pp. 643-658, 1974.

[7] G.C. Goodwin and K.S. Sin, *Adaptive Filtering Prediction and Control.* Prentice-Hall, Englewood Cliffs, New Jersey, 1984.

[8] K.S. Narendra and Y.H. Lin, "Design of stable model reference adaptive controllers," in *Applications of Adaptive Control,* K.S. Narendra and R.V. Monopoli, Eds., Academic Press, Ncw York, 1980.

[9] R. Ortega, P. Albertos, and R. Lozano-Leal, "Adaptive stabilization of discrete-time systems using linear periodically time varying controllers," Proc. 27th Conf. Decision and Control, pp. 1866-1870, Austin, Texas, December 1988.

[10] R. Lozano-Leal, "Robust adaptive regulation without persistent excitation," IEEE Trans. Automatic Control, vol. 34, no. 12, pp. 1260-1267, December 1989.

[11] A. Das, J.L. Berg, G.A. Norris, D.F. Cossey, T.J. Strange III, and W.T. Schlaedgel, "ASTREX - A Unique test bed for CSI research," Proc. 29th IEEE Conference on Decision and Control, Honolulu, Hawaii, pp. 2018-2023, December 1990.

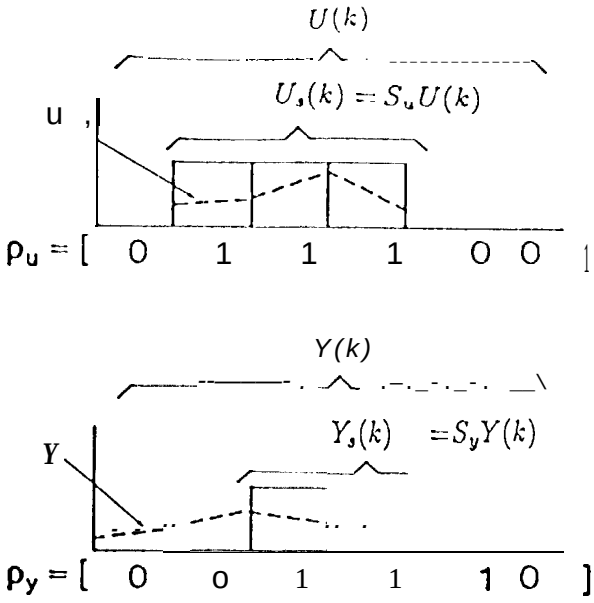

Figure 1: Partial horizon vectors U_s and Y_s defined from windows ρ_u and ρ_y

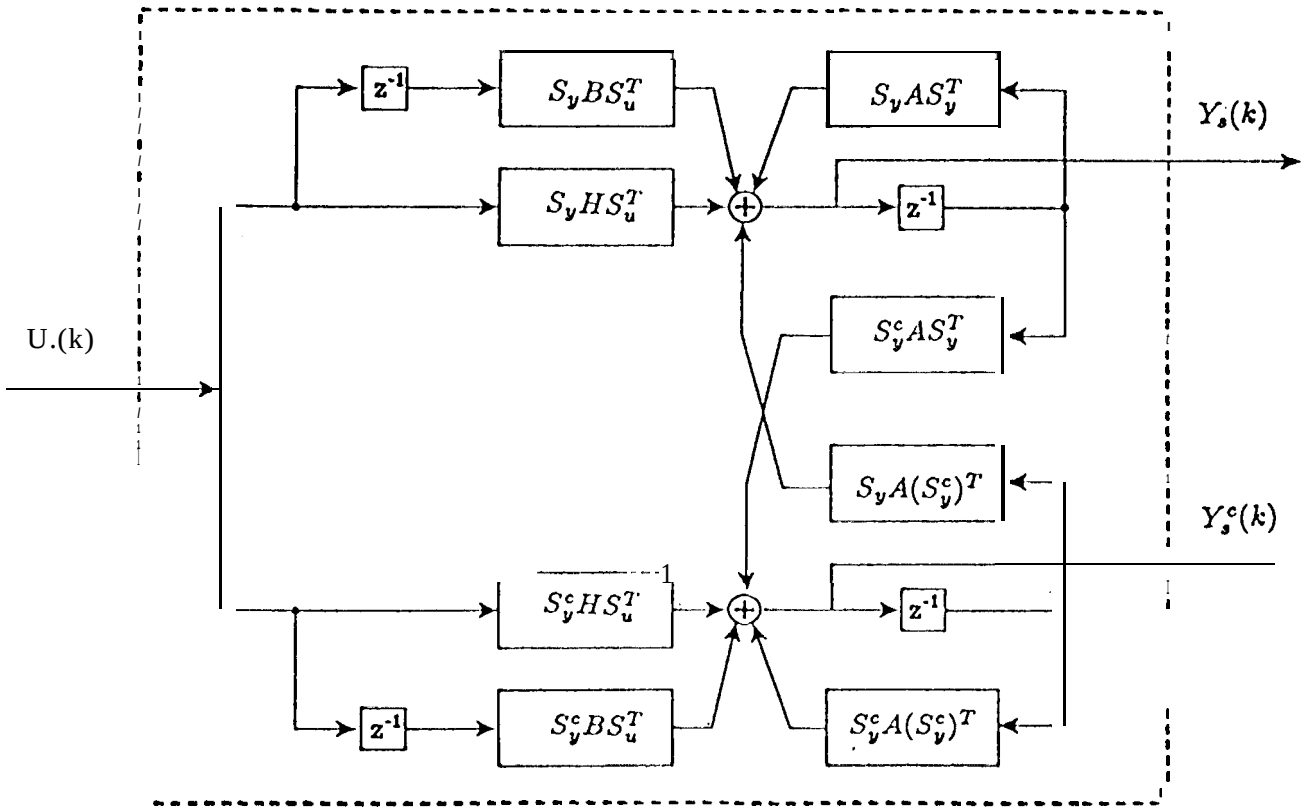

Figure 2: System Model for Generalized Lifting

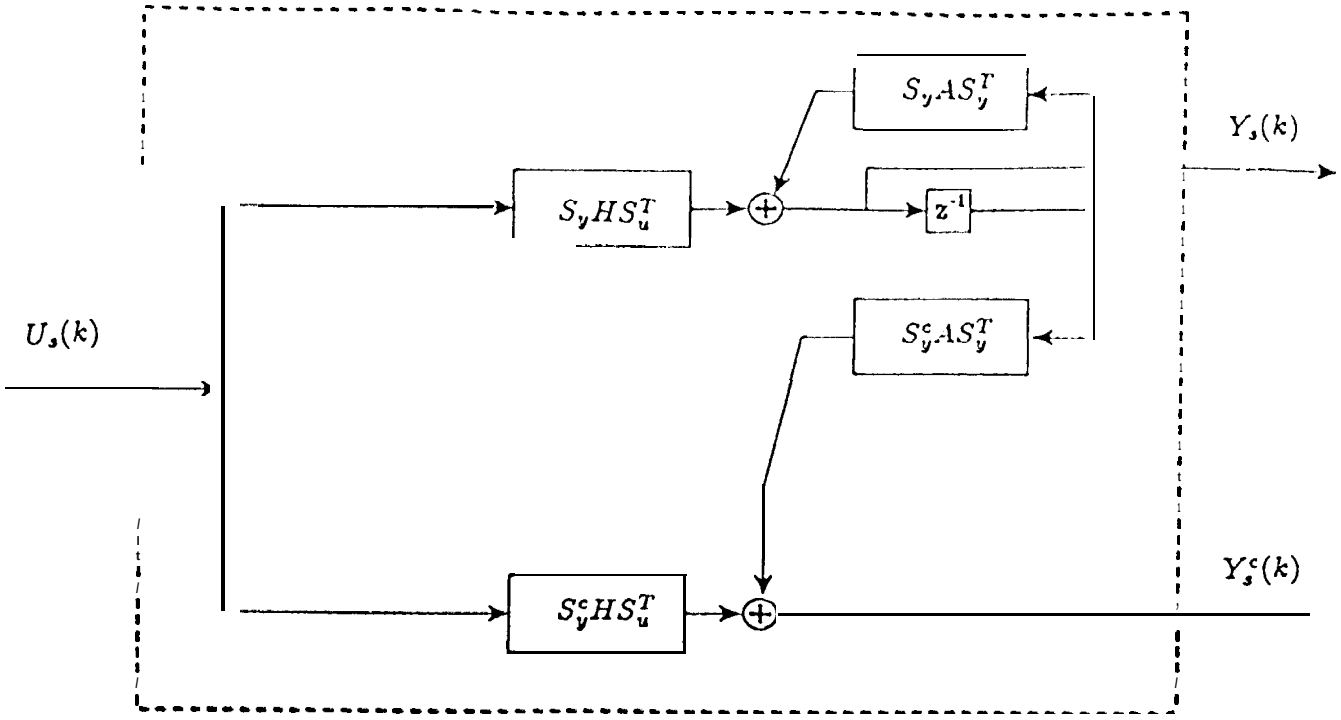

Figure 3: System Model for Extended Horizon Lifting

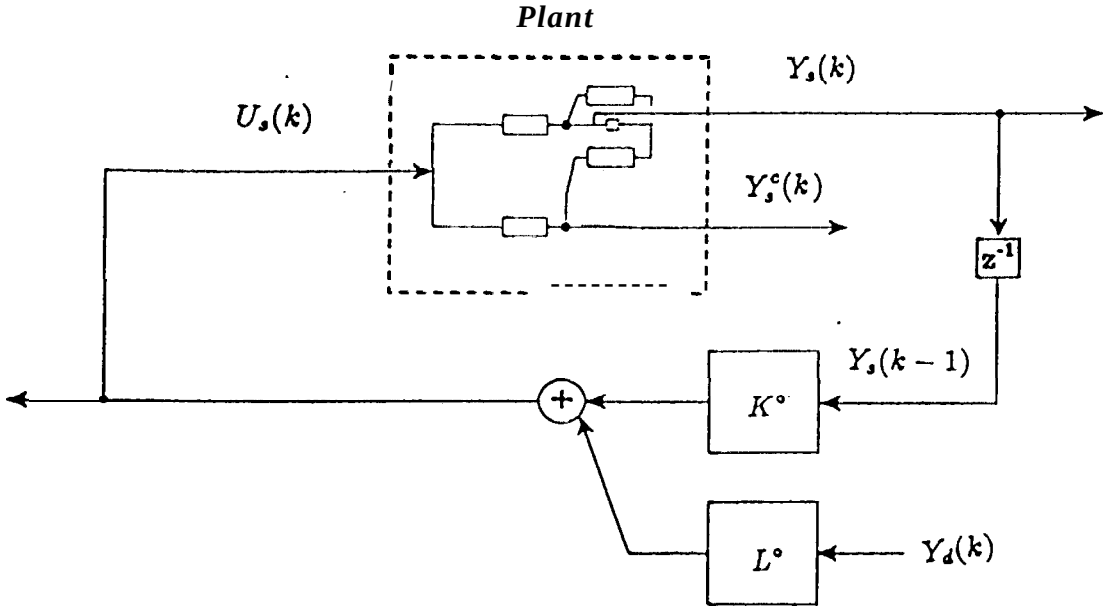

Figure 4: Zero Annihilation Periodic (ZAP) control architecture

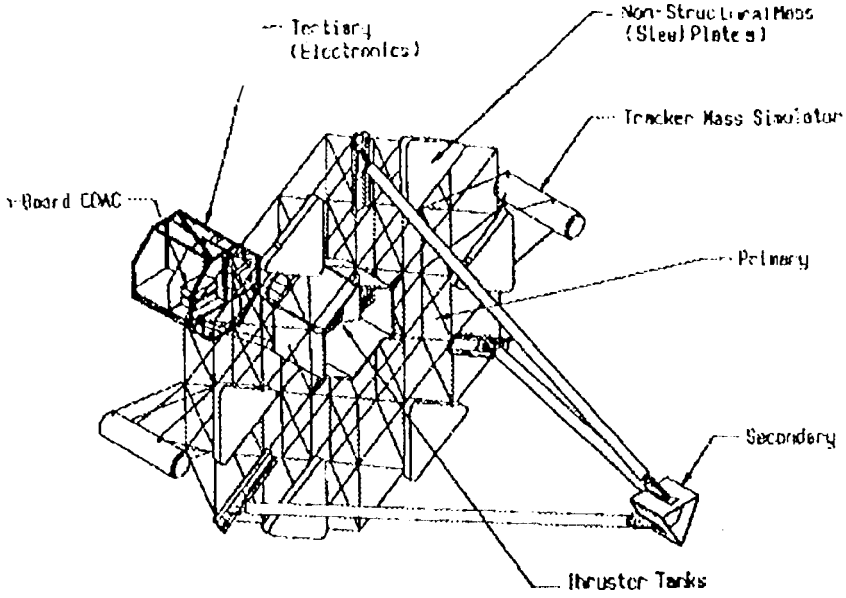

Figure 5: The ASTREX facility

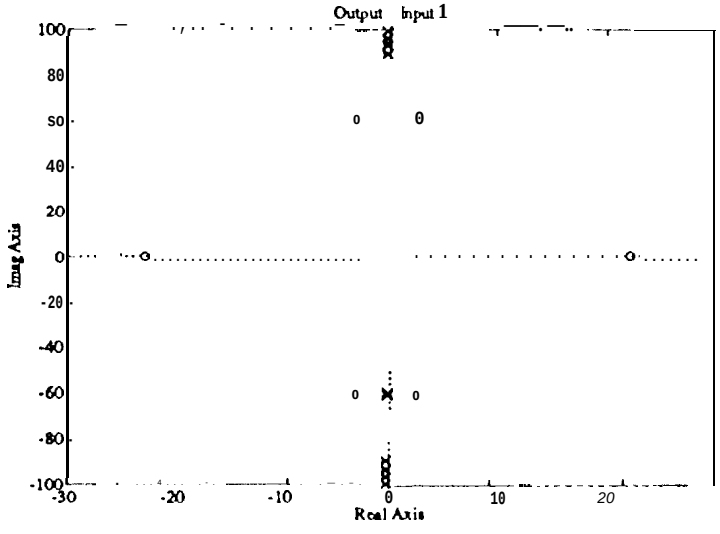

Figure 6: Pole-zero locations for transfer function y_1/u_1.

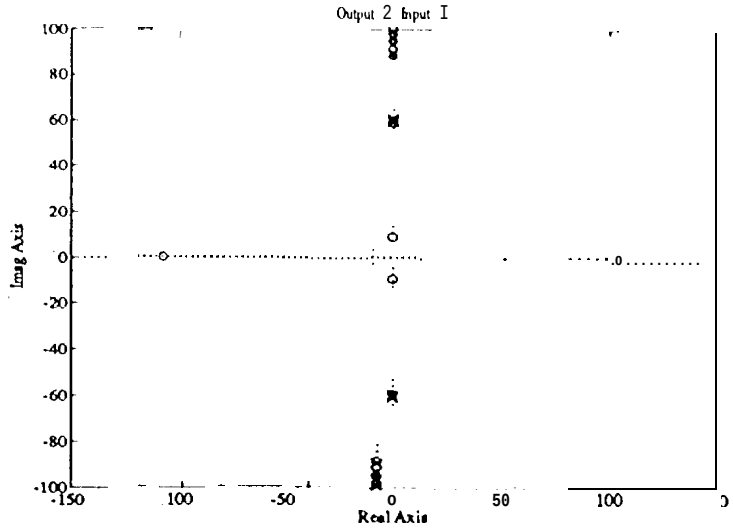

Figure 7: Pole-zero locations for transfer function y_2/u_1.

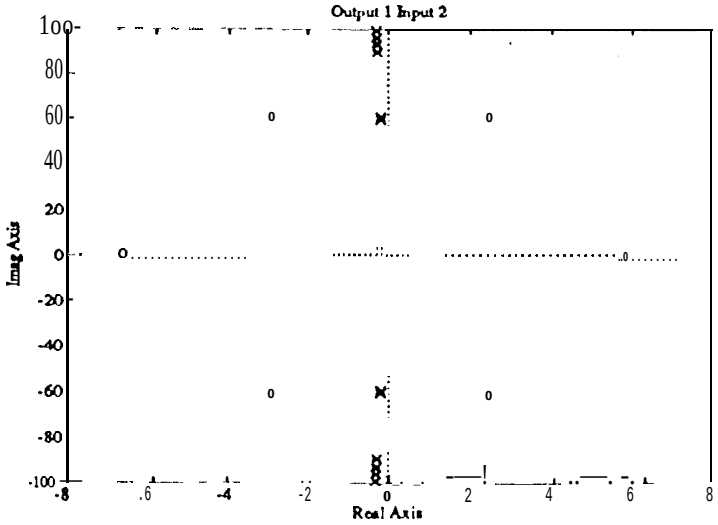

Figure 8: Pole-zero locations for transfer function y_1/u_2.

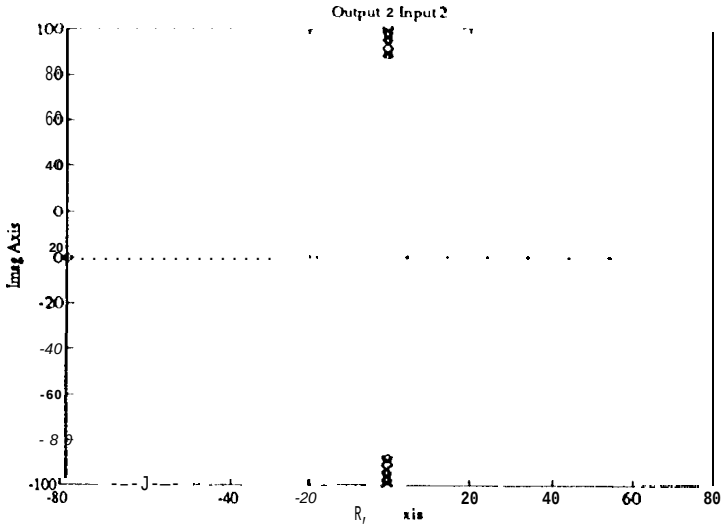

Figure 9: Pole-zero locations for transfer function y_2/u_2.

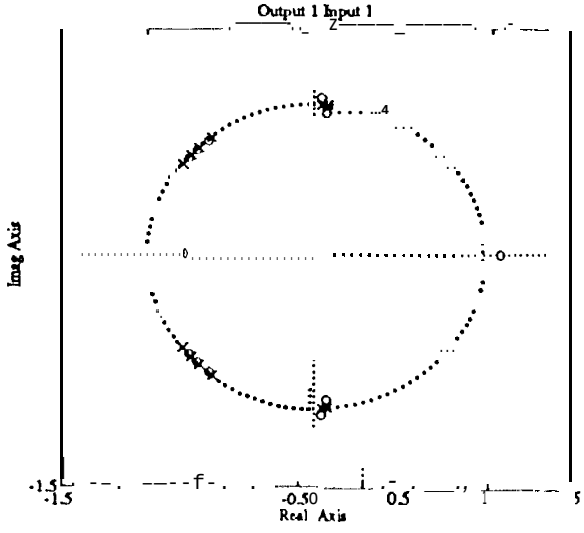

Figure 10: Pole-zero locations for channel 1-1 (discrete-time).

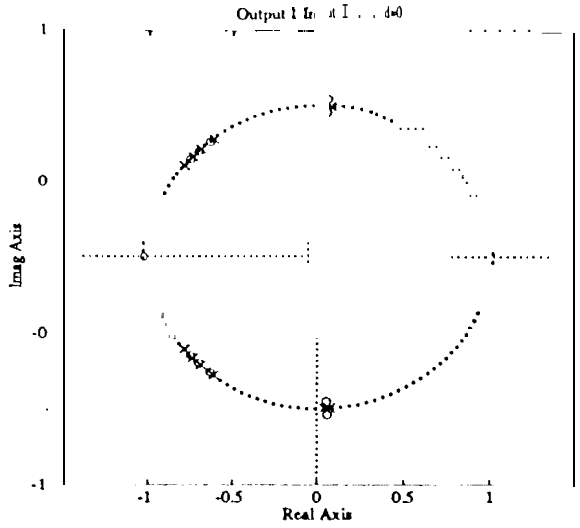

Figure 11: Pole-zero locations with d=- O.

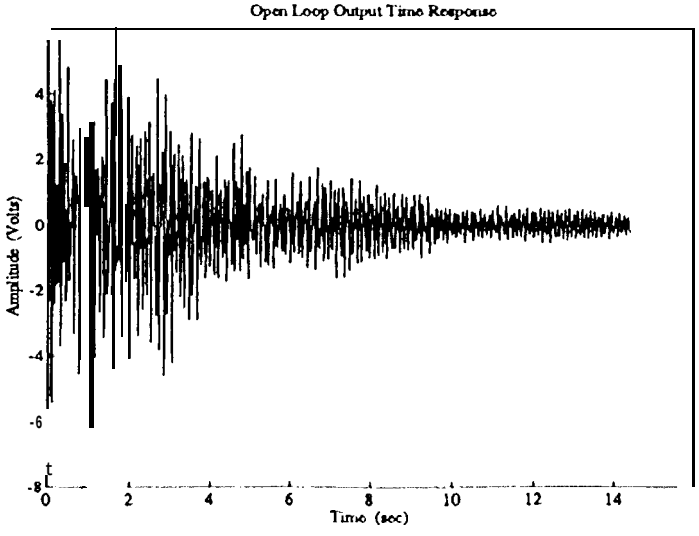

Figure 12: Open loop time response.

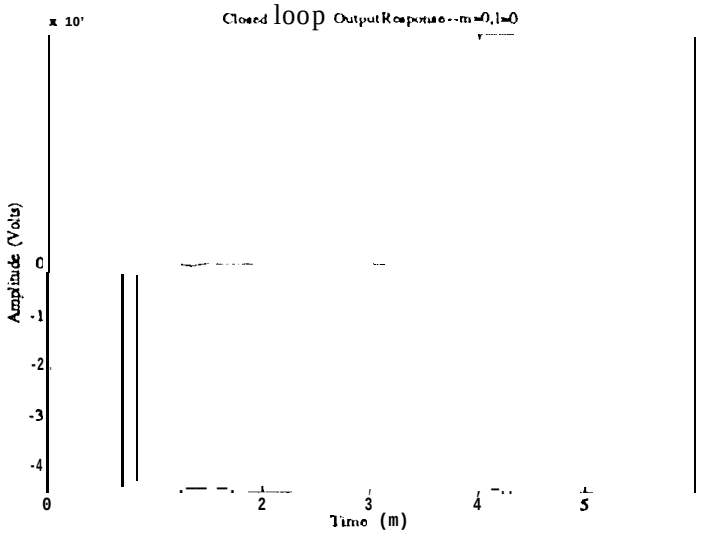

Figure 13: Closed loop output response for $\ell = 0$

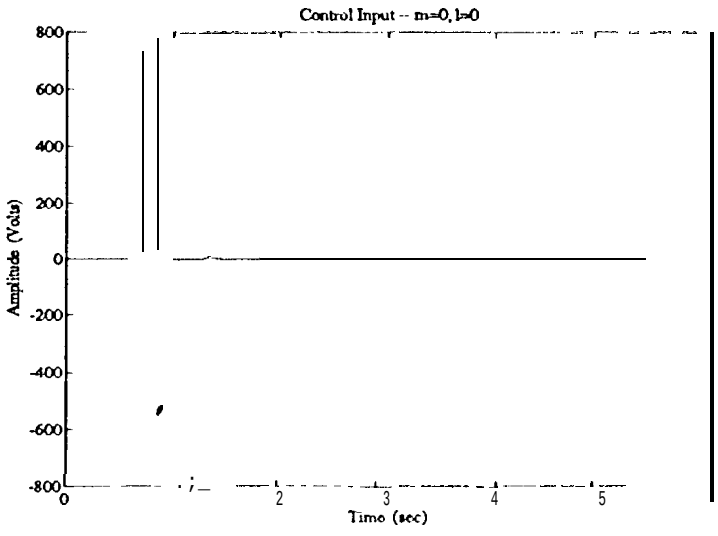

Figure 14: Control Input for $\ell = 0$

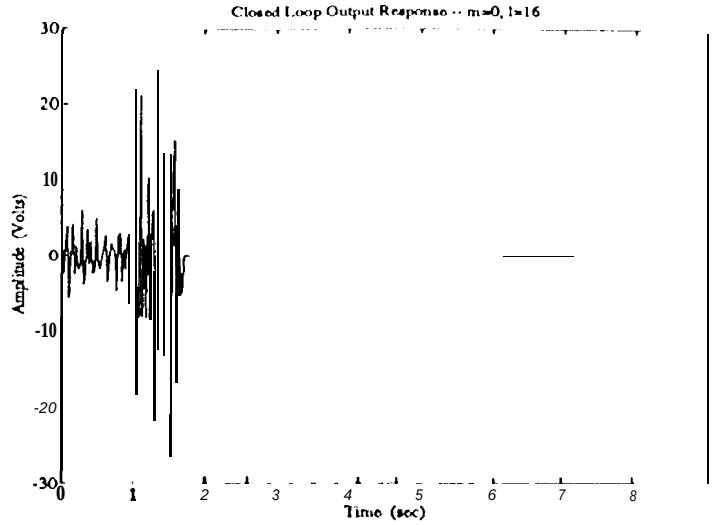

Figure 15: Closed loop output response for $\ell = 16$

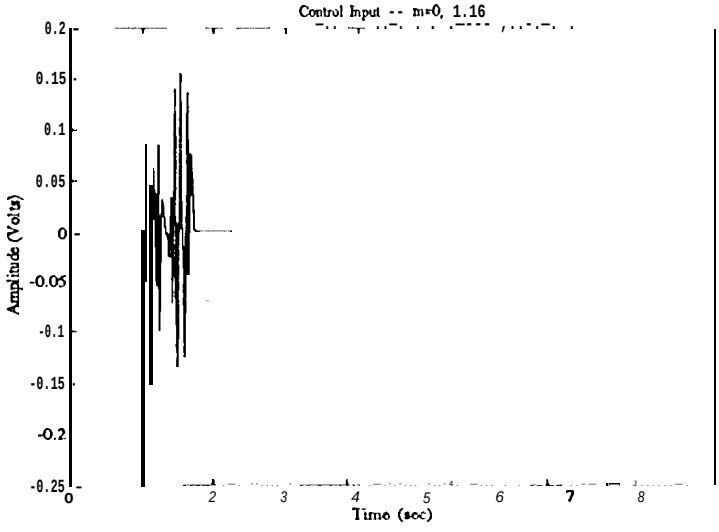

Figure 16: Control input for $\ell = 16$

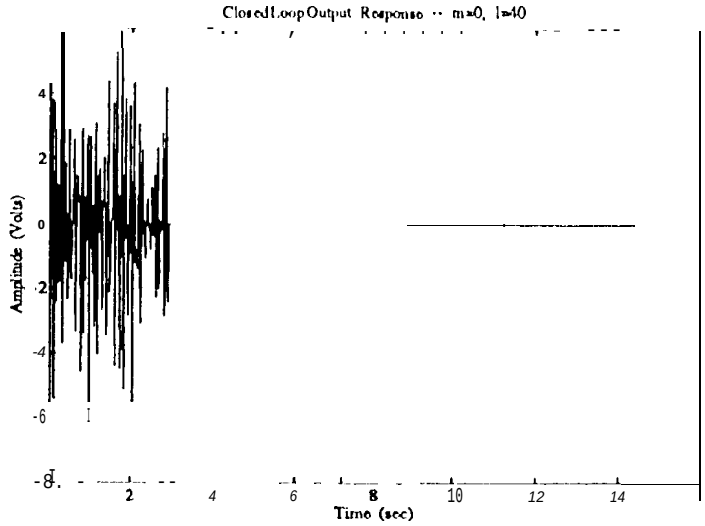

Figure 17: Closed loop output response for $\ell = 40$

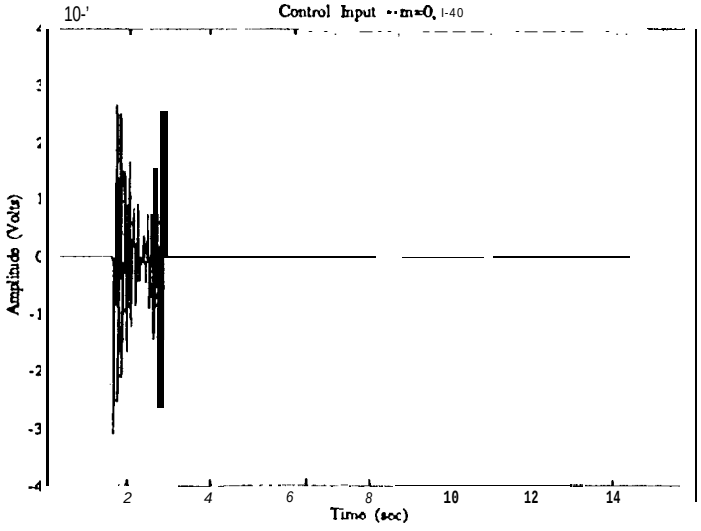

Figure 18: Control Input for $\ell = 40$

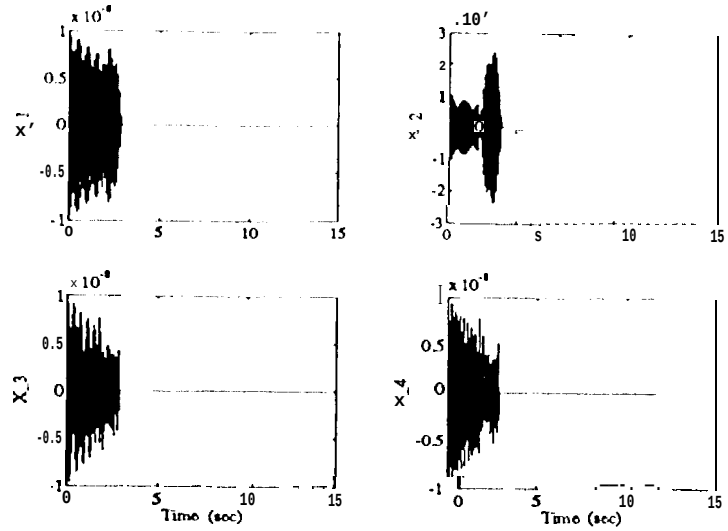

Figure 19: System states x_1-x_4 for $\ell = 40$

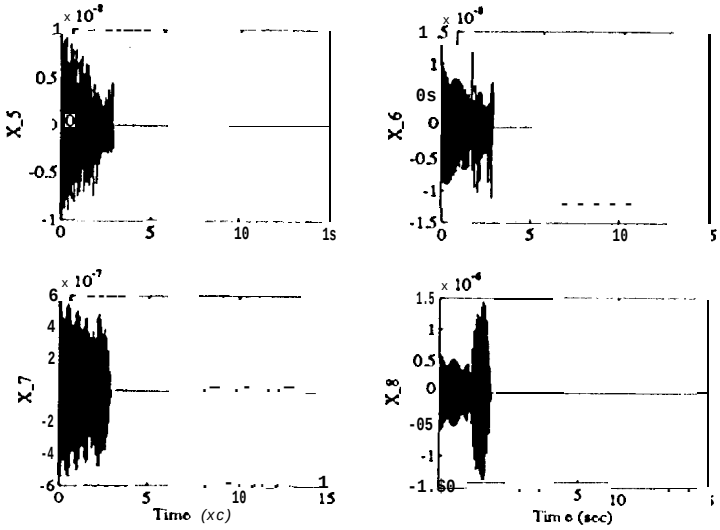

Figure 20: System states x_5-x_8 for $\ell = 40$

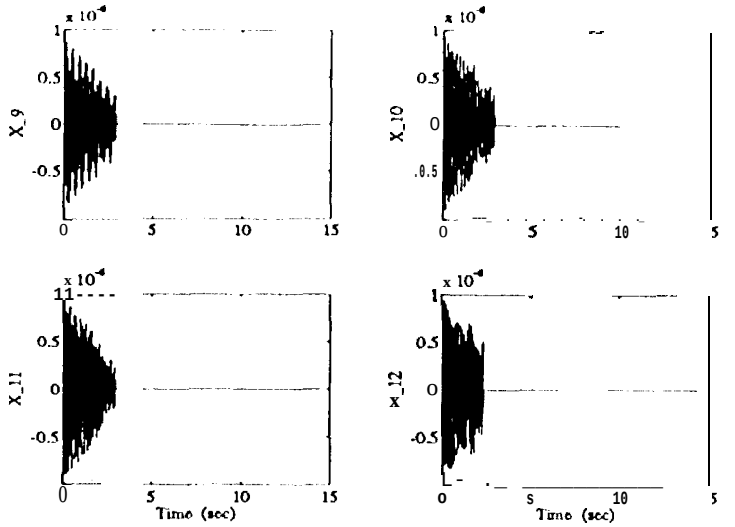

Figure 19: System states x_9-x_12 for $\ell = 40$